

Journal of  
**Applied Remote Sensing**

**Sensitivity studies for atmospheric  
carbon dioxide retrieval from  
atmospheric infrared sounder  
observations**

Mandi Zhou  
Jiong Shu  
Ci Song  
Wei Gao

# Sensitivity studies for atmospheric carbon dioxide retrieval from atmospheric infrared sounder observations

Mandi Zhou,<sup>a,b</sup> Jiong Shu,<sup>a</sup> Ci Song,<sup>a</sup> and Wei Gao<sup>a,c,d</sup>

<sup>a</sup>East China Normal University, Institute of Climate Change, and ECNU-CSU Joint Research Center for New Energy and the Environment, Key Laboratory of Geographic Information Science, 500 Dongchuan Road, Shanghai 200241, China

[jshu@geo.ecnu.edu.cn](mailto:jshu@geo.ecnu.edu.cn)

<sup>b</sup>China University of Geoscience, 388 Lumo Road, Wuhan 430074, China

<sup>c</sup>Colorado State University, Department of Ecosystem Science and Sustainability, Fort Collins, Colorado 80523

<sup>d</sup>Colorado State University, Natural Resource Ecology Laboratory, Fort Collins, Colorado 80523

**Abstract.** The atmospheric infrared sounder (AIRS) exhibits great potential for providing atmospheric observation data for long-term regional and global carbon-cycle studies, which are essential for understanding the uncertainty of climate change. The sensitivity of global atmospheric CO<sub>2</sub> retrieval from the AIRS observations by quantifying errors related to CO<sub>2</sub> measurements in the infrared spectrum is investigated. A line-by-line radiative transfer model is used to evaluate the effects of atmospheric temperature profile, water vapor profile, and ozone (O<sub>3</sub>) data on the accuracy of CO<sub>2</sub> measurements under five standard atmospheric models. The analytical results indicate that temperature, water vapor, and O<sub>3</sub> are important factors, which have great influences on the sensitivity of atmospheric CO<sub>2</sub> retrieval from the AIRS observations. The water vapor is the most important factor in the tropics, whereas the temperature represents major interference for multitude and subarctic regions. The results imply that precise measurements of temperature, water vapor, and O<sub>3</sub> can improve the quality of atmospheric CO<sub>2</sub> data retrieved from the AIRS observations. © The Authors. Published by SPIE under a Creative Commons Attribution 3.0 Unported License. Distribution or reproduction of this work in whole or in part requires full attribution of the original publication, including its DOI. [DOI: [10.1117/1.JRS.8.083697](https://doi.org/10.1117/1.JRS.8.083697)]

**Keywords:** sensitivity; CO<sub>2</sub>; retrieval.

Paper 13157 received May 10, 2013; revised manuscript received Oct. 1, 2013; accepted for publication Dec. 3, 2013; published online Jan. 6, 2014.

## 1 Introduction

The atmosphere is a superb integrator of spatiotemporally variable surface fluxes. The complexity of global and regional carbon cycles in surface fluxes leads to uncertainty in climate forecasting. The distribution of CO<sub>2</sub> in the atmosphere, and its time evolution, can thus be used to quantify surface fluxes. A satellite-based remote sounding instrument capable of measuring the long-term global distributions of CO<sub>2</sub> would greatly improve our ability to obtain the spatio-temporal variability of atmospheric CO<sub>2</sub> concentrations.<sup>1,2</sup>

Satellite measurements of the global atmospheric CO<sub>2</sub> distribution would record its continuous change, which could provide not only a long time series that is stable over wide regions, but also ground-to-aerial three-dimensional information regarding atmospheric composition. Advanced infrared (IR) sounders, particularly the atmospheric infrared sounder (AIRS) aboard the Aqua satellite and the Infrared Atmospheric Sounding Instrument (IASI) aboard the Metop satellite,<sup>3</sup> have been approved to retrieve mid-troposphere CO<sub>2</sub> concentration data. The scanning imaging absorption spectrometer for atmospheric chartography (SCIAMACHY)<sup>4</sup> aboard the European Environmental Satellite (ENVISAT) is a spectrometer designed to measure the surface concentrations of CO<sub>2</sub> because the channels sensitive to the near-IR are used for retrieval. The Greenhouse Gases Observing Satellite (GOSAT) was launched on January 23, 2009,

and its task is to monitor global atmospheric levels of greenhouse gases from space.<sup>5</sup> The orbiting carbon observatory (OCO) was specially equipped by the United States with a high-resolution spectroscopic instrument for CO<sub>2</sub> observations.<sup>6</sup> Unfortunately, the OCO failed to launch in 2009.<sup>3</sup> Currently, only the AIRS can provide stable long-term data on the global distribution of CO<sub>2</sub>. Therefore, simulated AIRS data were used to investigate the sensitivity of CO<sub>2</sub> retrieval with high precision. Researchers have applied various methods to retrieve CO<sub>2</sub> data using AIRS data.<sup>7-14</sup>

Because most of the variability in atmospheric CO<sub>2</sub> occurs in the planetary boundary layer, the CO<sub>2</sub> variability related to sinks and sources can be well represented by measurements of the total CO<sub>2</sub> column. Such measurements should be precise enough to resolve the CO<sub>2</sub> seasonal variability and horizontal gradients averaged over an atmospheric model grid box (e.g., 1 deg × 1 deg) and time scale (e.g., monthly) typical for climate studies and should be accurate enough to resolve long-term trends. For a column average, the mixing ratio gradients over horizontal scales of ~1000 km are typically 0.3% to 0.5% [i.e., 1 to 2 parts per million by volume (ppmv)]. The column measurement goal of 1-ppmv precision on a time scale of 1 month has been shown to improve surface source and sink estimates significantly in model studies.<sup>15</sup>

Radiance measurements from space can reflect not only CO<sub>2</sub> absorption but also other atmospheric factors, such as different atmospheric temperatures and pressures. Satellites are expected to provide a promising new source of CO<sub>2</sub> data by 2020. However, for column-integrated CO<sub>2</sub> measurements to be useful for source and sink inversions, the requirements on the measurements are stringent.<sup>16</sup> Moreover, little work on the sensitivity of atmospheric CO<sub>2</sub> retrieval from the AIRS observations has been reported.

It is well known that the increase in CO<sub>2</sub> concentration contributes to global climate change. In this study, the focus on atmospheric CO<sub>2</sub> change is through the response of radiance from the AIRS bands in relation to the responses of other variables. The dependence of the radiance sensitivity on the atmospheric temperature profile, water vapor profile, and O<sub>3</sub> data of different locations is also considered. This dependence produces the largest error source in the reverse accuracy of the CO<sub>2</sub> column concentration, except for those error sources caused while measuring with instrument characteristics. Therefore, the present sensitivity study of global atmospheric CO<sub>2</sub> retrieval from the AIRS observations will help to improve the understanding of uncertainty about climate change.

## 2 Measurement Strategies

### 2.1 Ground-Based Validation of the AIRS CO<sub>2</sub> Product

The AIRS instrument has been orbiting the earth on NASA's Aqua satellite in a sun-synchronous near-polar orbit since 2002. For the first time, it affords us the ability to retrieve CO<sub>2</sub> concentrations globally over land, ocean, and polar regions during the daytime and nighttime, even in the presence of clouds. The accuracy is better than 2 ppmv (i.e., <0.5%), without relying on *a priori* or background information.<sup>8</sup> An earlier study<sup>8</sup> compared the monthly seasonal variations of the AIRS retrievals to those of airborne measurements<sup>17</sup> for the period between September 2002 and March 2004. This comparison showed an agreement of  $0.43 \pm 1.20$  ppmv. Further comparisons have been performed with collocated *in situ* observations available for the period from September 2002 to July 2011.<sup>7</sup>

The satellite data for this article come from NASA's official AIRS mid-troposphere CO<sub>2</sub> product site ([http://airs.jpl.nasa.gov/AIRS\\_CO2\\_Data/](http://airs.jpl.nasa.gov/AIRS_CO2_Data/)). Hyperspectral data of low instrument noise from the AIRS have been used to produce global profiles of temperature and water vapor as well as carbon dioxide and other trace gases. The tropospheric CO<sub>2</sub> products are derived by binning the Level 2 standard retrievals in a grid that is 2 deg in latitude by 2.5 deg in longitude over daily, 8-day, and monthly time spans.<sup>7</sup>

Ground-based measurements can provide the CO<sub>2</sub> concentration with high precision. The World Meteorological Organization (WMO), the U.S. National Oceanic and Atmospheric Administration (NOAA), the Meteorological Service of Canada (MSC), and the Japanese National Institute for Environmental Studies (NIES) have built numerous ground-based CO<sub>2</sub>

observation stations throughout the world<sup>18,19</sup> to obtain information about variations in CO<sub>2</sub>. Data from ground-based and aerial CO<sub>2</sub> measurements are available at the WMO World Data Centre for Greenhouse Gases (WMO WDCGG) web site (<http://gaw.kishou.go.jp/wdcgg/wdcgg.html>).<sup>18</sup>

The above-mentioned agencies provide measurements from a total of ~201 baseline observatories, fixed sites, and tall towers, complemented by measurements from ships and aircraft. Although the *in situ* measurements are highly accurate, the distribution in space and time is necessarily somewhat limited for global process studies.<sup>15</sup>

In this article, 123 *in situ* data are selected to validate the quality of the AIRS CO<sub>2</sub> product. These data cover the period from September 2002 to July 2011, which is the same period as covered by the AIRS data. Figure 1 compares the AIRS CO<sub>2</sub> products with the *in situ* observations for September 2002 to July 2011. This comparison shows that the AIRS results are consistent with the ground-based observations. Figure 1 provides the average bias, standard deviation, and correlation coefficients for both the ground-based and satellite observations over the years. The correlation coefficients are higher than 0.8 for most stations from 60°S to 30°N. Further, the bias is lower than 3 ppmv, and the monthly average standard deviation is <3 ppmv.

The correlation coefficient is lower than 0.5 for the areas from 30°N to 90°N. That is, the northern hemisphere shows a lower correlation than the southern hemisphere, because the concentration of human activities is higher in the northern hemisphere than in the vast sparsely populated areas of the southern hemisphere. The bias is ~5 ppmv, and the monthly average standard deviation is generally within 6 ppmv (though some individual sites have large deviations).

The validation results show that the AIRS mid-troposphere CO<sub>2</sub> product is consistent with ground-based and aerial measurements at various latitudes. The error is mainly for northern latitudes from 30°N to 60°N, followed by the Arctic.

## 2.2 Sensitivity of AIRS CO<sub>2</sub> Retrieval

### 2.2.1 Algorithm for CO<sub>2</sub> concentration retrieval

The AIRS is a high-spectral-resolution spectrometer with 2378 bands in the thermal IR (3.7 to 15.4 μm) and 4 bands in the visible wavelengths (0.4 to 1.0 μm). Data from the AIRS and its companion instrument, the Advanced Microwave Sounding Unit (AMSU), are combined to

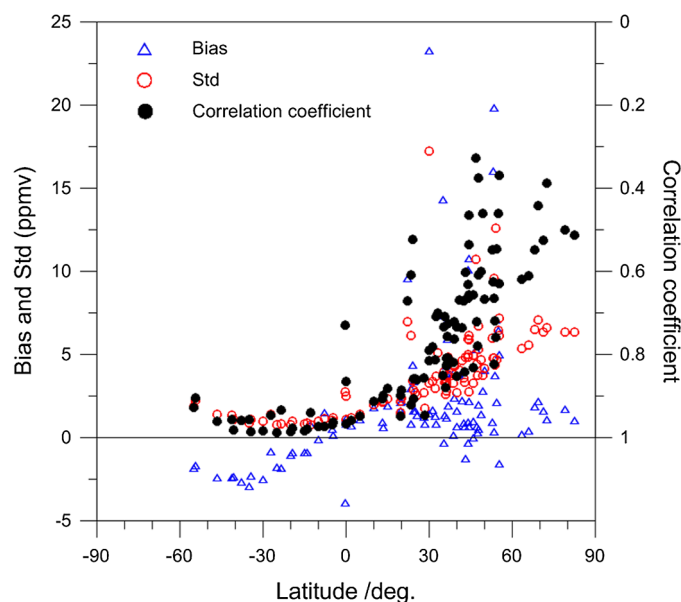


**Fig. 1** Error comparisons between atmospheric infrared sounder (AIRS) products and *in situ* observations.

eliminate the effects of clouds.<sup>19</sup> The resulting AIRS Level 2 products include these cloud-cleared IR radiances and retrieved profiles of atmospheric temperature, water vapor, and O<sub>3</sub> with a nominal spatial resolution of 45 km at nadir. The AIRS/AMSU/Humidity Sounder for Brazil (HSB) instrument suite is constructed to obtain atmospheric temperature profiles to an accuracy of 1 K for every 1-km layer in the troposphere and 1 K for every 4-km layer in the stratosphere up to an altitude of 40 km. The accuracy of the temperature profile in the troposphere matches that achieved by radiosondes launched from ground stations. In conjunction with the temperature profiles, the AIRS instrument suite obtains water vapor profiles to an accuracy of 20% in the 2-km layer of the lower troposphere and to an accuracy of 20% to 60% in the upper troposphere.<sup>20</sup>

The tropospheric CO<sub>2</sub> products released by the AIRS project through the Goddard Earth Sciences Data and Information Services Center (GES DISC) are derived by means of the vanishing partial derivatives (VPDs) method of Chahine et al.<sup>8</sup> The VPD method is based on the Gauss method for finding a local minimum on an  $n$ -dimensional surface. The Gauss method is based on a general property of the total differential of a multivariate function: at the point of a local minimum (or maximum), the first partial derivatives of the function with respect to each unknown must individually vanish.

The VPD CO<sub>2</sub> solution is obtained by an iterative process that minimizes the RMS difference between the Level 2 cloud-cleared radiances and the forward-computed radiances from the Level 2 profiles retrieved for selected CO<sub>2</sub> channels in the 15- $\mu$ m band. The process begins with the AIRS Level 2 atmospheric state and CO<sub>2</sub> climatology and then separately perturbs the temperature, water vapor, O<sub>3</sub>, and CO<sub>2</sub>. The solution is obtained at the point where the partial derivatives of the CO<sub>2</sub> channels with respect to temperature, water vapor, O<sub>3</sub>, and CO<sub>2</sub> are individually equal to zero (minimized).

Evaluation of the relative sensitivity of each channel to temperature, water vapor, O<sub>3</sub>, and CO<sub>2</sub> leads to the choice of the spectral range used in the VPD retrieval. The range 690 to 725 cm<sup>-1</sup> is well suited for selecting the channel set to retrieve the CO<sub>2</sub> mixing ratio.<sup>17</sup> Table 1 summarizes the IR channels whose cloud-cleared radiances are used in the VPD retrieval of tropospheric CO<sub>2</sub>. An evaluation of the sensitivity of the CO<sub>2</sub> retrieval to temperature, water vapor, and O<sub>3</sub> can help us to understand the sources of retrieval errors.

### 2.2.2 Sensitivity of CO<sub>2</sub> concentration retrieval

Radiance measurements from the space in a CO<sub>2</sub> absorption band can reflect the total CO<sub>2</sub> column. Variations in the vertical temperature profile, the water vapor profile, and the distribution of interfering gases as the satellite instrument moves will add uncertainties to the CO<sub>2</sub> measurements.<sup>1</sup> To study the effects of these variations on the retrieval of CO<sub>2</sub> columns, the AIRS measurements are simulated in the spectral range 690 to 725 cm<sup>-1</sup>. The strong CO<sub>2</sub> emission band at 15  $\mu$ m is used to derive atmospheric temperature profiles, with the assumption that the CO<sub>2</sub> concentration throughout the atmosphere is fixed. The sensitivity of space-observed radiance to emission temperature in this band is much greater than the sensitivity to the CO<sub>2</sub> concentration. In addition, water vapor and the O<sub>3</sub> column cause significant interference within this band.

The radiative transfer model used for atmospheric absorption in this study is called the line-by-line radiative transfer model (LBLRTM).<sup>21</sup> The LBLRTM is an accurate, efficient, and well-established line-by-line algorithm that is widely used in studies of atmospheric radiation and remote sensing to validate band models, generate fast-forward models in retrieval processes, and simulate radiance for high-spectral-resolution sensor designs. The high-resolution

**Table 1** List of channels used for the vanishing partial derivatives iterative solution.

Channel	192	198	209	210	212	214	215
Wavenumber (cm <sup>-1</sup> )	704.436	706.137	709.279	709.566	710.141	710.716	711.005
Channel	216	217	218	228	239	250	—
Wavenumber (cm <sup>-1</sup> )	711.293	711.582	711.871	714.773	717.994	721.244	—

transmission molecular absorption database is used as input to the LBLRTM.<sup>22</sup> The Voigt profile is used for absorption line shapes to include both collisional- and Doppler-broadening processes throughout the column of the atmosphere.

Models of five standard atmospheres are used for atmospheric profiles with extensions to 100 km.<sup>23</sup> The atmospheric radiance in the spectral range 690 to 725  $\text{cm}^{-1}$  is shown in Fig. 2(a). The baseline atmospheric  $\text{CO}_2$  mixing ratio is set to 380 ppmv, and the satellite view is set to nadir.

According to the accuracies of the AIRS products, the temperature profiles have an accuracy of 1 K for every 1-km layer, the atmospheric water vapor profile has an accuracy of 20% in 2-km layers, and there are 10% errors in the  $\text{O}_3$  column. Based on the error quantification presented here, the change produced in the measured radiance by these errors is compared with the change in the  $\text{CO}_2$  concentration. Then the maximum uncertainty in the retrieved  $\text{CO}_2$  concentration is produced by these errors under the five standard atmospheric models.

### 3 Results

#### 3.1 Spectral Resolution

A scanning function is used, which can simulate the slit function of a grating spectrometer to convolve the monochromatic radiances calculated line-by-line. The radiance measurement of the reflected IR wavelength at high spectral resolution results in a high sensitivity to atmospheric  $\text{CO}_2$  change. Thus, a balance in the spectral resolution and the radiance sensitivity is required of instrumentation for  $\text{CO}_2$  measurements.

The effects of spectral resolution on radiance and radiance sensitivity are presented in Figs. 2(b)–2(f), from the highest possible resolution of the model ( $\sim 0.00015 \text{ cm}^{-1}$ , black lines) to the spectral resolution of AIRS ( $\lambda/\Delta\lambda = 1200$ , colored lines). The results show that the AIRS resolution, unlike the model resolution, is adequate for  $\text{CO}_2$  spectral features, can maintain a moderate radiance level, and has good radiance sensitivity.

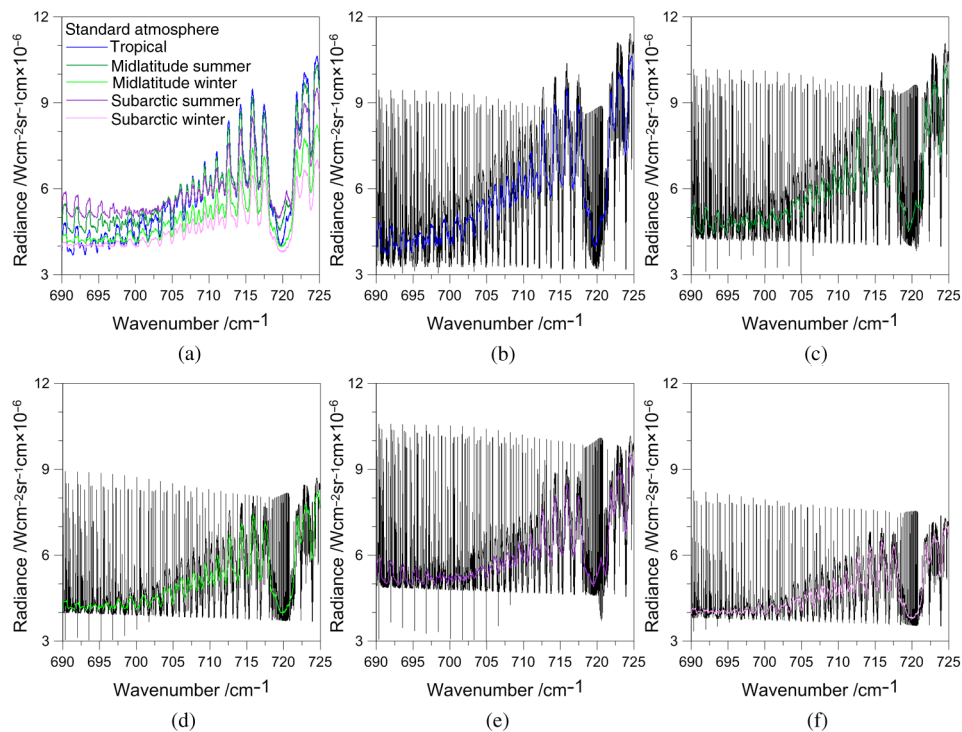


**Fig. 2** Radiance at different spectral resolutions under five different standard atmospheric models: (a) all standard atmospheric models, (b) tropical, (c) midlatitude summer, (d) midlatitude winter, (e) subarctic summer, and (f) subarctic winter.

### 3.2 Radiance Sensitivity for CO<sub>2</sub> Change

Altitude has an important effect on the CO<sub>2</sub> absorption linewidth through pressure broadening.<sup>15</sup> Figure 3 shows the change produced in the measured radiance by a 1 ppmv increase in the CO<sub>2</sub> concentration in each 1-km layer of the atmosphere. The measured radiance decreases with a 1-ppmv increase in the CO<sub>2</sub> concentration because the transmittance decreases as the CO<sub>2</sub> concentration increases. Furthermore, the vertical sensitivity calculated for a 1-ppmv CO<sub>2</sub> increase in each 1-km layer is shown in Fig. 4 for the 13 AIRS channels used in the NOAA retrievals under the five different standard atmospheric models. The AIRS mid-troposphere CO<sub>2</sub> is well mixed, because the channels used for retrieval are sensitive to altitudes of ~10 km, which provide the strongest contributions to the measured radiance. The changes in radiance are mainly caused by the variations in atmospheric CO<sub>2</sub> concentration at altitudes of 20 km or less.

Moreover, the AIRS weighting functions have a tail that extends into the stratosphere, especially in the polar regions, where the tropopause is lower. The stratospheric air is colder than that of the troposphere by an amount that varies with latitude.<sup>24–28</sup> As can be observed in Fig. 4, an increase in latitude produces a negative change in radiance sensitivity. Additionally, the radiance sensitivity is greater in summer than in winter. Overall, greater radiance sensitivity leads to a more precise retrieval of the CO<sub>2</sub> concentration data.

The change in the measured radiance was also calculated for a 1-ppmv increase in the CO<sub>2</sub> column for the 13 AIRS channels used in the NOAA retrievals under the five different standard atmospheric models. The results include the variance and sensitivity of the upwelling radiance at the top of the atmosphere, as shown in Table 2. The band at 711.005 cm<sup>-1</sup> is particularly sensitive in all five standard atmospheric models, and the maximum value of the radiance sensitivity is 0.078%. Comparing the values of radiance sensitivity under the five standard atmospheric models, it can be seen that an increase in latitude corresponds to a decrease in radiance sensitivity, whereas the radiance sensitivity is greater in summer than in winter.

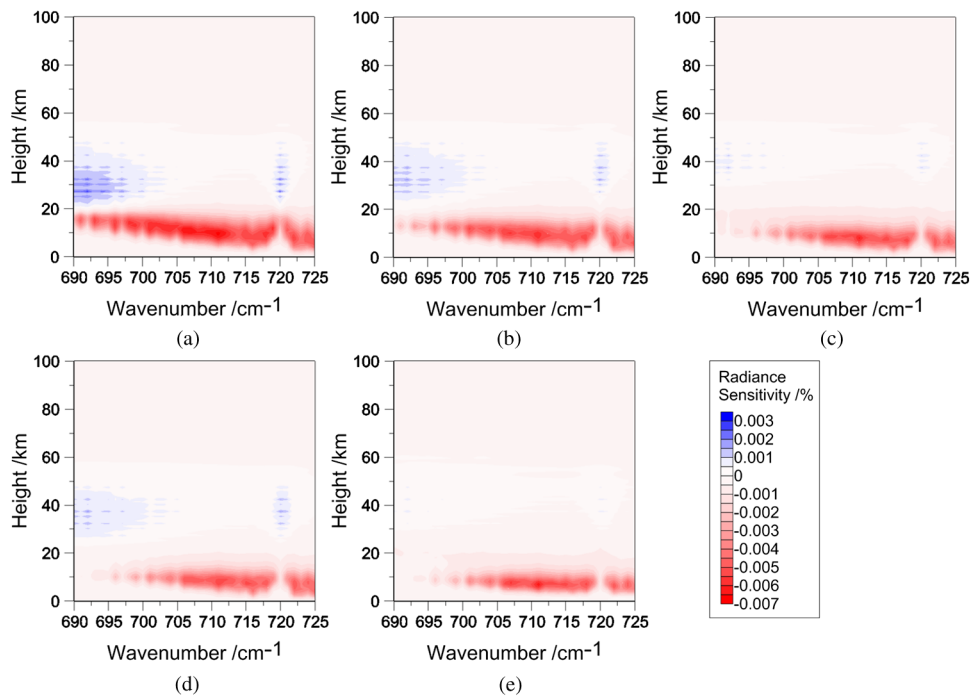


**Fig. 3** CO<sub>2</sub> Jacobians for a 1-ppmv layer perturbation under five different standard atmospheric models: (a) tropical, (b) midlatitude summer, (c) midlatitude winter, (d) subarctic summer, and (e) subarctic winter.

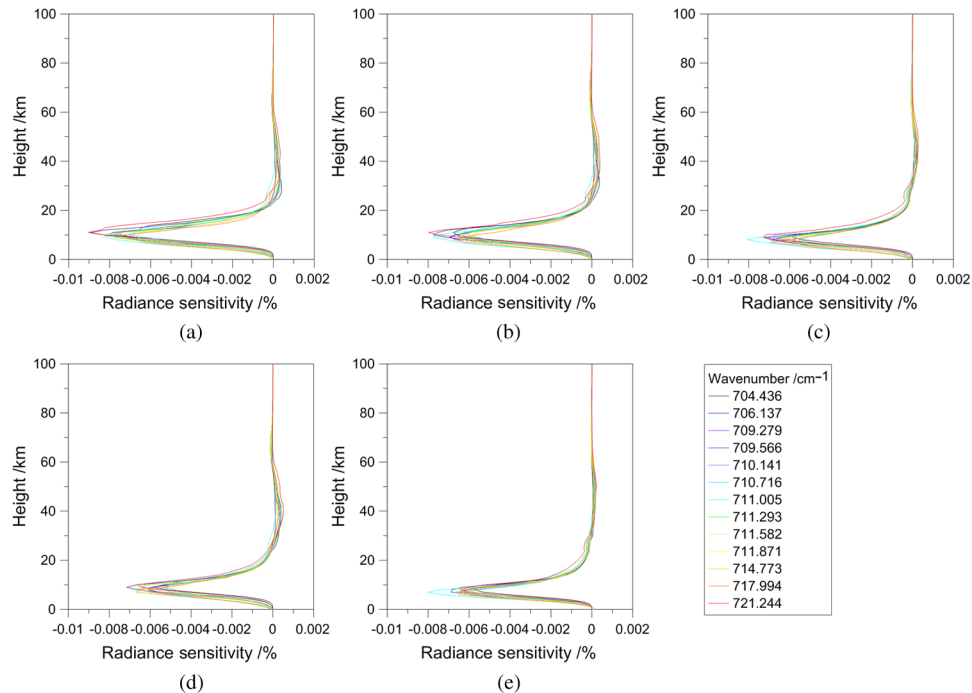


**Fig. 4** CO<sub>2</sub> Jacobians for a 1-ppmv layer perturbation for the 13 AIRS channels used in the National Oceanic and Atmospheric Administration (NOAA) retrievals under five different standard atmospheric models: (a) tropical, (b) midlatitude summer, (c) midlatitude winter, (d) subarctic summer, and (e) subarctic winter.

### 3.3 Temperature Dependence

Temperature greatly affects the CO<sub>2</sub> absorption coefficient in terms of line strength, line shape, and even line position. Thus, the amount of back-to-space radiance in the IR greatly depends on the atmospheric temperature, even though the dependence is much weaker than in the bands for temperature profile retrieval.<sup>15</sup>

The AIRS/AMSU/HSB instrument suite is able to measure atmospheric temperature profiles to an accuracy of 1 K for every 1-km layer in the troposphere and 1 K for every 4-km layer in the stratosphere up to an altitude of 40 km. In this study, a 1-K temperature deviation was added to each layer of the five standard atmospheric models. Such a deviation is likely for temperature profile retrieval errors when matching the observed radiances with computed radiances. Figure 5 shows the radiance changes in percent for the 13 AIRS channels used in the NOAA retrievals after the 1-K temperature error was introduced into the temperature profile under the five standard atmospheric models. The overall influence of the temperature retrieval error is <0.2%, which is significantly smaller than the change due to a 1% CO<sub>2</sub> change.

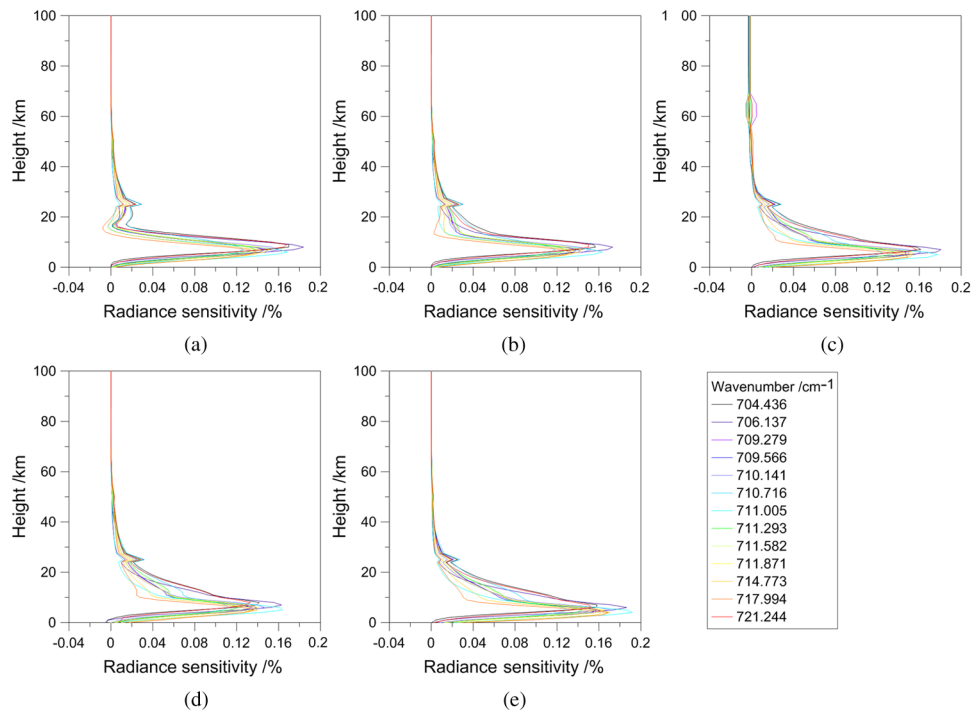
The channels used for retrieval are sensitive to altitudes of ~10 km, which provide the strongest contributions to the measured radiance. These altitudes are similar to those of the CO<sub>2</sub> radiance sensitivity, resulting in a greater interference for CO<sub>2</sub> concentration retrieval. The 706.137-cm<sup>-1</sup> band is the most sensitive, but the change produced in the measured radiance by a temperature increase of 1 K is negligible above 40 km in the atmosphere. Furthermore, the tropical and subarctic regions have greater radiance sensitivity than the midlatitude areas, while the radiance sensitivity at each latitude is greater in winter than in summer because of the seasonal dependence, especially in the subarctic region.

Figure 6 shows the variations in measured radiance caused by temperature errors (top curve) and the change in CO<sub>2</sub> concentration (bottom curve) under the five standard atmospheric models. It can be observed that the change in the measured radiance is a function of the 1-K increase in each 1-km layer of the atmosphere. In the troposphere, the measured radiance is more sensitive to temperature changes. As observed in Fig. 6, the maximum sensitivity to a 1-K change in each 1-km layer of the atmosphere is approximately three times the sensitivity to a 1-ppmv change in



**Table 2** Variations and sensitivities of measured radiance for a 1-ppmv CO<sub>2</sub> change in five different standard atmospheres.

Wavenumber (cm <sup>-1</sup> )	Tropical			Midlatitude summer			Midlatitude winter			Subarctic summer			Subarctic winter		
	ΔRadiance (W cm <sup>-2</sup> sr <sup>-1</sup> cm × 10 <sup>-9</sup> )	Radiance sensitivity (%)	ΔRadiance (W cm <sup>-2</sup> sr <sup>-1</sup> cm × 10 <sup>-9</sup> )	Radiance sensitivity (%)	ΔRadiance (W cm <sup>-2</sup> sr <sup>-1</sup> cm × 10 <sup>-9</sup> )	Radiance sensitivity (%)	ΔRadiance (W cm <sup>-2</sup> sr <sup>-1</sup> cm × 10 <sup>-9</sup> )	Radiance sensitivity (%)	ΔRadiance (W cm <sup>-2</sup> sr <sup>-1</sup> cm × 10 <sup>-9</sup> )	Radiance sensitivity (%)	ΔRadiance (W cm <sup>-2</sup> sr <sup>-1</sup> cm × 10 <sup>-9</sup> )	Radiance sensitivity (%)	ΔRadiance (W cm <sup>-2</sup> sr <sup>-1</sup> cm × 10 <sup>-9</sup> )	Radiance sensitivity (%)	ΔRadiance (W cm <sup>-2</sup> sr <sup>-1</sup> cm × 10 <sup>-9</sup> )
704.436	3.71	0.067	3.15	0.056	2.24	0.046	2.33	0.042	1.86	0.042	1.86	0.042	1.86	0.042	1.86
706.137	4.53	0.074	3.96	0.065	2.89	0.055	3.15	0.053	2.41	0.051	2.41	0.051	2.41	0.051	2.41
709.279	4.33	0.067	3.75	0.058	2.97	0.055	3.07	0.049	2.42	0.049	2.42	0.049	2.42	0.049	2.42
709.566	4.21	0.066	3.65	0.057	2.91	0.054	2.91	0.047	2.41	0.048	2.41	0.048	2.41	0.048	2.41
710.141	4.35	0.068	3.87	0.061	3.03	0.056	3.14	0.051	2.45	0.050	2.45	0.050	2.45	0.050	2.45
710.716	3.99	0.066	3.51	0.057	2.49	0.048	2.65	0.044	2.04	0.043	2.04	0.043	2.04	0.043	2.04
711.005	5.62	0.078	5.19	0.073	3.91	0.066	4.26	0.064	3.25	0.060	3.25	0.060	3.25	0.060	3.25
711.293	4.16	0.068	3.61	0.058	2.90	0.055	2.82	0.047	2.39	0.049	2.39	0.049	2.39	0.049	2.39
711.582	4.06	0.064	3.51	0.055	2.68	0.050	2.85	0.046	2.26	0.046	2.26	0.046	2.26	0.046	2.26
711.871	4.39	0.067	3.82	0.059	2.88	0.053	3.20	0.051	2.43	0.049	2.43	0.049	2.43	0.049	2.43
714.773	4.62	0.066	4.19	0.061	3.24	0.056	3.49	0.053	2.68	0.051	2.68	0.051	2.68	0.051	2.68
717.994	4.59	0.064	4.10	0.059	3.36	0.056	3.49	0.052	2.79	0.051	2.79	0.051	2.79	0.051	2.79
721.244	4.66	0.084	3.87	0.069	2.90	0.061	2.79	0.051	2.35	0.053	2.35	0.053	2.35	0.053	2.35



**Fig. 5** Temperature Jacobians for a 1-K layer perturbation for the 13 AIRS channels used in the NOAA retrievals under five different standard atmospheric models: (a) tropical, (b) midlatitude summer, (c) midlatitude winter, (d) subarctic summer, and (e) subarctic winter.

CO<sub>2</sub>. If the curves in Fig. 6 are integrated and compared with the CO<sub>2</sub> column sensitivities (Table 2), a 1-K decrease in the atmospheric temperature over the entire profile is found to produce a change in measured radiance comparable with that produced by a 1% increase in the CO<sub>2</sub> concentration (listed in Table 3 for all channels).

In summary, an analysis of the sources of uncertainty in the proposed CO<sub>2</sub> radiometer was performed. The analysis shows that the most important potential source of error is uncertainty in the temperature profile. The maximum sensitivity to temperature, at 3.82 ppmv, is found in the 704.436-cm<sup>-1</sup> band. This value is at least 1-ppmv higher than those in other bands. Moreover, higher latitude leads to more serious temperature interference. The effect that temperature error has on the CO<sub>2</sub> retrieval is less in summer than in winter at the same latitude. Therefore, a good knowledge of the atmospheric temperature profile is required as ancillary data in CO<sub>2</sub> retrieval.

### 3.4 Water Vapor Interference

Water vapor has only slight absorption in the band 690 to 725 cm<sup>-1</sup>, which requires attention when channels are selected for CO<sub>2</sub> retrieval. Fortunately, most of the water vapor line centers in this band are not aligned with the CO<sub>2</sub> line centers. The calculated difference in CO<sub>2</sub> sensitivity between atmospheres with and without water vapor is negligible for most lines. However, atmospheric water vapor can significantly modify air density, reinforcing the abovementioned requirement for dry-air surface pressure measurements. However, for some wet-summer areas, such as the tropics and midlatitudes, major interference from highly variable atmospheric water vapor is a great concern for this IR band.

Figure 7 shows that the lowest layers of the atmosphere provide the strongest contributions to the measured radiance. The 714.773-cm<sup>-1</sup> band is the most sensitive, and most of the change in radiance is contributed by the variation in the water vapor concentration of the atmosphere below 15 km.

Although this spectral interval was chosen partly to reduce the interference of water vapor in the measured radiances, such interference remains a significant factor in the retrieval of CO<sub>2</sub> concentrations. The proposed measurement of atmospheric water vapor has an accuracy of

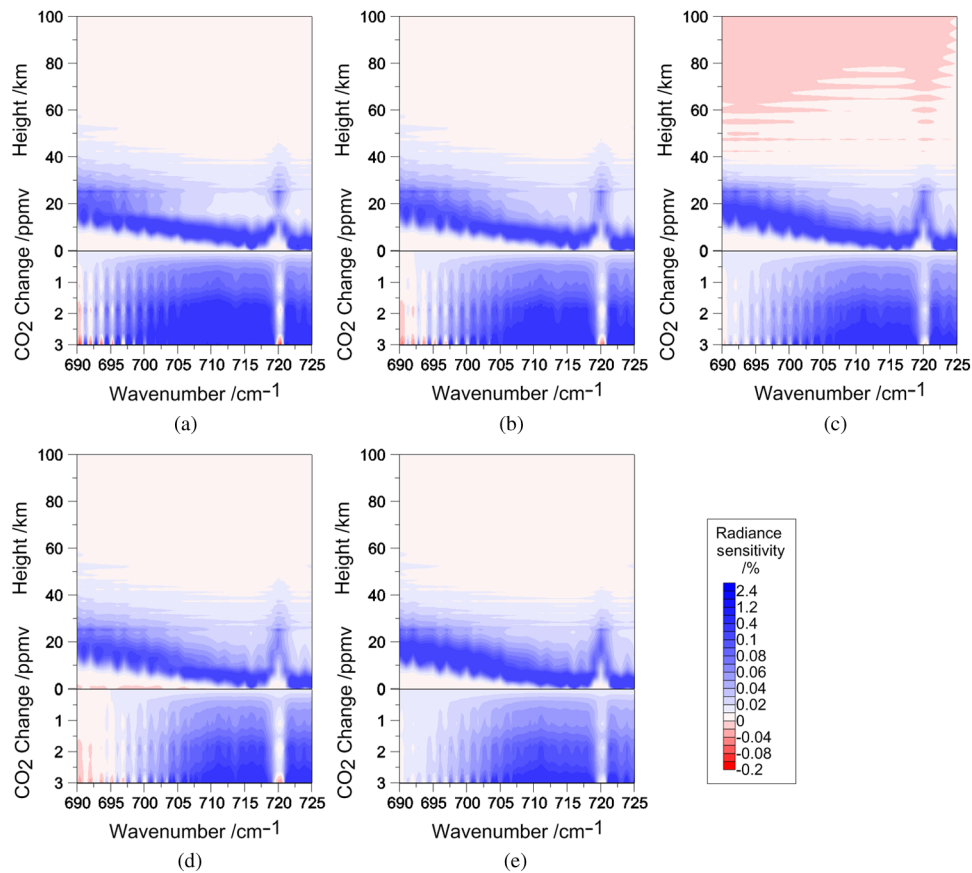


**Fig. 6** Variations in radiance caused by measured temperature errors (top curve) and the change in CO<sub>2</sub> concentration (bottom curve) under five different standard atmospheric models: (a) tropical, (b) midlatitude summer, (c) midlatitude winter, (d) subarctic summer, and (e) subarctic winter.

20% every 2-km layers. Figure 8 shows the fractional change in the measured radiance as a function of a 20% relative humidity decrease in each 2-km layer of the atmosphere, with respect to a standard relative humidity profile. The fractional changes in the measured radiance are <0.01% for the midlatitude winter and the subarctic region. Given this level of sensitivity to water vapor, the maximum errors for a CO<sub>2</sub> measurement precision of 0.5% are ~2.58, 2.63, 0.85, 1.36, and 0.12 ppmv for the tropics, midlatitude summer, midlatitude winter, subarctic summer, and subarctic winter, respectively (see Table 3). In relative terms, lower latitude areas have greater uncertainty than higher latitude areas, and summer has greater uncertainty than winter for a given latitude.

For water vapor, the column sensitivity is greatly determined by seasonal dependence, which is mostly a result of higher densities because of the greater amounts of water vapor in the atmosphere. However, the uncertainty for CO<sub>2</sub> concentration retrieval is generally <2 ppmv in summer and <1 ppmv in winter.

### 3.5 O<sub>3</sub> Interference

Interference in the measured radiance due to O<sub>3</sub> is a significant factor in the process of CO<sub>2</sub> retrieval. The radiance measured for the reflected IR wavelength results in a high sensitivity to O<sub>3</sub> change. Comparisons with O<sub>3</sub> radiosonde data have shown for the AIRS observations that such interference leads to errors as sizeable as -10% in the O<sub>3</sub> column of the stratosphere and yields an accuracy of 20% to 70% for the troposphere. The O<sub>3</sub> product of the AIRS has a bias of -11% to +3% compared with that of the total ozone mapping spectrometer.<sup>29-31</sup> The sensitivity of the measured radiance to the O<sub>3</sub> profile is presented in Fig. 9.

**Table 3** Uncertainty in CO<sub>2</sub> retrieval caused by temperature, water vapor, and O<sub>3</sub> errors under five different standard atmospheres.

Wavenumber (cm <sup>-1</sup> )	Tropical (ppmv)				Midlatitude summer (ppmv)				Midlatitude winter (ppmv)				Subarctic summer (ppmv)				Subarctic Winter (ppmv)			
	T	H <sub>2</sub> O	O <sub>3</sub>	Overall error	T	H <sub>2</sub> O	O <sub>3</sub>	Overall error	T	H <sub>2</sub> O	O <sub>3</sub>	Overall error	T	H <sub>2</sub> O	O <sub>3</sub>	Overall error	T	H <sub>2</sub> O	O <sub>3</sub>	Overall error
704.436	2.54	0.19	0.58	3.32	2.82	0.23	0.80	3.85	3.49	0.17	1.56	5.22	3.39	0.21	0.61	4.21	3.82	0.05	1.58	5.45
706.137	2.49	0.39	0.75	3.64	2.68	0.70	0.96	4.34	3.26	0.31	1.42	5.00	3.04	0.39	0.83	4.27	3.69	0.12	1.40	5.20
709.279	2.24	0.70	1.69	4.63	2.44	0.98	2.20	5.63	2.75	0.39	3.01	6.16	2.82	0.37	1.98	5.18	3.31	0.08	3.17	6.56
709.566	2.23	0.73	1.64	4.59	2.42	0.97	2.06	5.45	2.74	0.36	2.87	5.97	2.86	0.38	1.92	5.16	3.25	0.07	2.99	6.31
710.141	2.36	0.41	0.96	3.73	2.52	0.58	1.16	4.26	2.88	0.23	1.66	4.77	2.87	0.26	0.99	4.12	3.46	0.06	1.74	5.26
710.716	1.91	1.73	1.03	4.67	2.06	1.88	1.39	5.33	2.59	0.61	2.40	5.60	2.55	0.73	1.34	4.62	3.02	0.08	2.52	5.62
711.005	2.17	1.66	1.06	4.89	2.23	1.89	1.30	5.41	2.70	0.68	1.85	5.23	2.57	0.73	1.26	4.56	3.19	0.11	1.91	5.21
711.293	2.03	0.78	0.54	3.35	2.21	1.10	0.74	4.05	2.46	0.47	1.16	4.09	2.60	0.44	0.71	3.75	2.94	0.10	1.27	4.31
711.582	2.23	0.90	1.03	4.16	2.44	1.12	1.40	4.96	2.90	0.40	2.14	5.44	2.83	0.38	1.26	4.47	3.38	0.07	2.16	5.61
711.871	2.24	0.95	1.40	4.59	2.43	1.14	1.82	5.39	2.90	0.41	2.69	6.00	2.73	0.40	1.53	4.66	3.38	0.07	2.67	6.12
714.773	2.16	2.58	1.38	6.12	2.27	2.63	1.80	6.69	2.74	0.85	2.50	6.09	2.62	1.15	1.77	5.54	3.35	0.11	2.62	6.09
717.994	2.16	2.58	1.50	6.23	2.28	2.40	1.89	6.58	2.65	0.82	2.60	6.06	2.61	1.36	1.80	5.76	3.29	0.11	2.77	6.17
721.244	2.00	0.23	0.69	2.92	2.17	0.49	0.89	3.55	2.59	0.26	1.38	4.23	2.62	0.27	0.77	3.66	2.86	0.05	1.41	4.33
Maximum	2.54	2.58	1.69	6.23	2.82	2.63	2.20	6.69	3.49	0.85	3.01	6.16	3.39	1.36	1.98	5.76	3.82	0.12	3.17	6.56

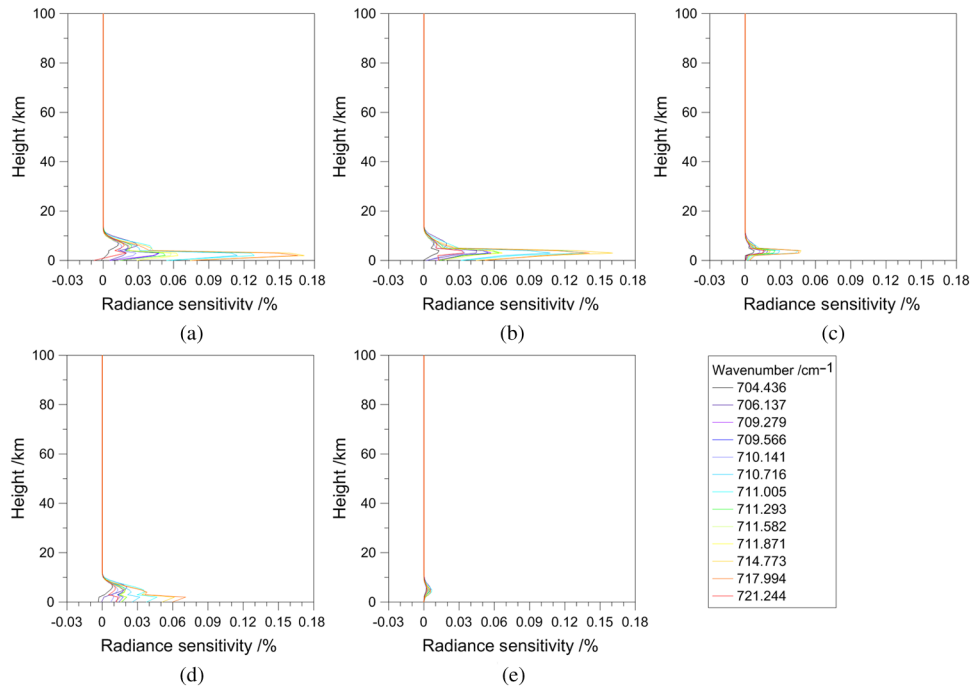


**Fig. 7** Water vapor Jacobians for a 20% layer perturbation for the 13 AIRS channels used in the NOAA retrievals under five different standard atmospheric models: (a) tropical, (b) midlatitude summer, (c) midlatitude winter, (d) subarctic summer, and (e) subarctic winter.

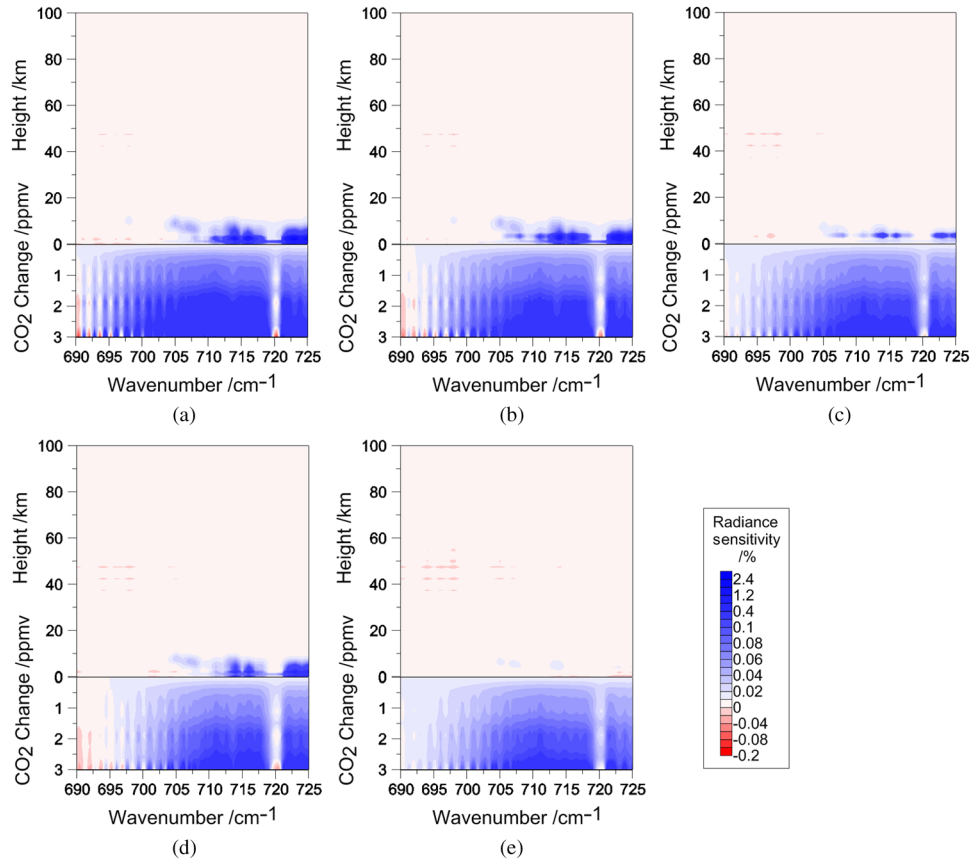


**Fig. 8** Variations caused by water vapor errors from observation under five standard atmospheric models: (a) tropical, (b) midlatitude summer, (c) midlatitude winter, (d) subarctic summer, and (e) subarctic winter.

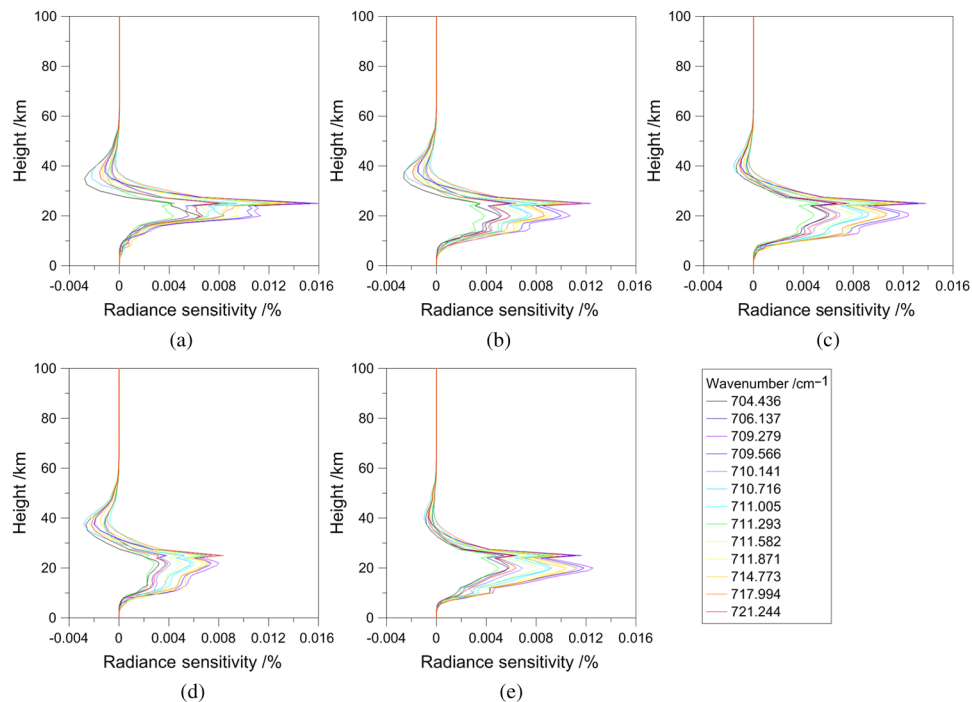


**Fig. 9**  $O_3$  Jacobians for a 10% layer perturbation for the 13 AIRS channels used in the NOAA retrieval under five different standard atmospheric models: (a) tropical, (b) midlatitude summer, (c) midlatitude winter, (d) subarctic summer, and (e) subarctic winter.

The channels used for retrieval are sensitive to stratospheric altitudes of  $\sim 20$  to  $30$  km, which provide the strongest contributions to the measured radiance. These altitudes are much greater than those of the  $CO_2$  radiance sensitivity, but the measured radiance produces fractional change by a 10% decrease of  $O_3$  in each 1-km layer of the atmosphere above 60 km. Tropical areas have greater radiance sensitivity than higher latitude areas, and the radiance sensitivity at each latitude is greater in winter than in summer because of the seasonal dependence, especially in the subarctic region.

In these IR channels, the sensitivity of measured radiance exhibits a 0.016% change by  $-10\%$  variation of  $O_3$  concentration (a reasonable level of variation in  $O_3$  over the globe). Given this level of sensitivity, the maximum errors in  $O_3$  concentration for  $CO_2$  measurements are  $\sim 1.69$ , 2.20, 3.01, 1.98, and 3.17 ppmv, respectively (see Table 3).

Another source of error is spectral interference from  $O_3$  in the  $709.279\text{-cm}^{-1}$  band. This interference has a minimal value of 1.69 ppmv in the tropics, and then increases to 3.17 ppmv when coupled with higher latitude areas and seasonal dependence. The value of the uncertainty is 1-ppmv higher in winter than in summer at the same latitude.

In summary, the three factors of temperature,  $O_3$ , and water vapor have great influences on the sensitivity of atmospheric  $CO_2$  retrieval from the AIRS observations. In particular, the most important factor in the tropics is water vapor, while temperature represents major interference for midlatitude and subarctic regions. Moreover, the maximum error in  $CO_2$  retrieval occurs for mid latitude regions under summer conditions.

## 4 Conclusions

The global sensitivity of atmospheric  $CO_2$  retrieval from the AIRS observations was investigated to quantify the largest error source at the IR wavelengths for global and regional carbon-cycle studies. To fully resolve the line features and obtain maximum radiance sensitivity, the results were calculated using the LBLRTM and presented at spectral resolution  $\lambda/\Delta\lambda = 1200$ , which is the typical linewidth of  $CO_2$  at standard temperature and pressure. The results show that temperature,  $O_3$ , and water vapor are important factors, which have great influences on the sensitivity of

atmospheric CO<sub>2</sub> retrieval from the AIRS observations. Specifically, the water vapor is the most important factor in the tropics, whereas the temperature represents major interference for mid-latitude and subarctic regions. Moreover, the maximum error caused by temperature, water vapor, and O<sub>3</sub> data in CO<sub>2</sub> retrieval occurs for midlatitude regions under summer conditions. The findings are in good agreement with those from the ground-based validation of the AIRS CO<sub>2</sub> products. Therefore, precise measurements of the water vapor profile, access to O<sub>3</sub> data, and good knowledge of the atmospheric temperature profile are important to reduce errors, especially in the CO<sub>2</sub> retrieval for midlatitude regions.

## Acknowledgments

This project was supported by the National Basic Research Program of China (No. 2010CB951603) and the Shanghai Science and Technology Support Program—Special for Expo (No. 10DZ0581600). The computation was supported by the High Performance Computer Center of East China Normal University.

## References

1. B. T. Tolton and D. Plouffe, “Sensitivity of radiometric measurements of the atmospheric CO<sub>2</sub> column from space,” *Appl. Opt.* **40**(9), 1305–1313 (2001), <http://dx.doi.org/10.1364/AO.40.001305>.
2. C. Crevoisier, A. Chedin, and N. A. Scott, “AIRS channel selection for CO<sub>2</sub> and other trace-gas retrievals,” *Q. J. Roy. Meteorol. Soc.* **129**(593), 2719–2740 (2003), <http://dx.doi.org/10.1256/qj.02.180>.
3. F. Cayla and P. Javelle, “IASI instrument overview: advanced and next-generation satellite,” *Proc. SPIE* **2583**, 271–281 (1995), <http://dx.doi.org/10.1117/12.228572>.
4. M. Buchwitz et al., “Carbon monoxide, methane and carbon dioxide columns retrieved from SCIAMACHY by WFM-DOAS: Year 2003 initial data set,” *Atmos. Chem. Phys.* **5**(12), 3313–3329 (2005), <http://dx.doi.org/10.5194/acp-5-3313-2005>.
5. A. Kuze et al., “Thermal and near infrared sensor for carbon observation Fourier-transform spectrometer on the greenhouse gases observing satellite for greenhouse gases monitoring,” *Appl. Opt.* **48**(35), 6716–6733 (2009), <http://dx.doi.org/10.1364/AO.48.006716>.
6. D. Crisp et al., “The orbiting carbon observatory (OCO) mission,” *Adv. Space Res.* **34**(4), 700–709 (2004), <http://dx.doi.org/10.1016/j.asr.2003.08.062>.
7. M. T. Chahine et al., “Satellite remote sounding of mid-tropospheric CO<sub>2</sub>,” *Geophys. Res. Lett.* **35**, L17807 (2008), <http://dx.doi.org/10.1029/2008GL035022>.
8. M. Chahine et al., “On the determination of atmospheric minor gases by the method of vanishing partial derivatives with application to CO<sub>2</sub>,” *Geophys. Res. Lett.* **32**, L22803 (2005), <http://dx.doi.org/10.1029/2005GL024165>.
9. A. A. Alkhaled et al., “A global evaluation of the regional spatial variability of column integrated CO<sub>2</sub> distributions,” *J. Geophys. Res.: Atmos.* **113**(D20) (2008), <http://dx.doi.org/10.1029/2007JD009693>.
10. R. J. Engelen et al., “Global observations of the carbon budget: 1 Expected satellite capabilities for emission spectroscopy in the EOS and NPOESS eras,” *J. Geophys. Res.* **106**(D17), 20055–20068 (2001), <http://dx.doi.org/10.1029/2001JD900223>.
11. R. J. Engelen and A. P. McNally, “Estimating atmospheric CO<sub>2</sub> from advanced infrared satellite radiances within an operational four-dimensional variational (4D-Var) data assimilation system: results and validation,” *J. Geophys. Res.* **110**(18), D18305 (2005), <http://dx.doi.org/10.1029/2005JD005982>.
12. R. J. Engelen, S. Serrar, and F. Chevallier, “Four-dimensional data assimilation of atmospheric CO<sub>2</sub> using AIRS observations,” *J. Geophys. Res.* **114**(3), D03303 (2009), <http://dx.doi.org/10.1029/2008JD010739>.
13. E. S. Maddy et al., “CO<sub>2</sub> retrievals from the atmospheric infrared sounder: methodology and validation,” *J. Geophys. Res.* **113**(11), D11301 (2008), <http://dx.doi.org/10.1029/2007JD009402>.

14. L. L. Strow and S. E. Hannon, "A 4-year zonal climatology of lower tropospheric CO<sub>2</sub> derived from ocean-only atmospheric infrared sounder observations," *J. Geophys. Res.* **113**(18), D18302 (2008), <http://dx.doi.org/10.1029/2007JD009713>.
15. J. Mao and S. R. Kawa, "Sensitivity studies for space-based measurement of atmospheric total column carbon dioxide by reflected sunlight," *Appl. Opt.* **43**(4), 914–927 (2004), <http://dx.doi.org/10.1364/AO.43.000914>.
16. I. Aben, O. Hasekamp, and W. Hartmann, "Uncertainties in the space-based measurements of CO<sub>2</sub> columns due to scattering in the Earth's atmosphere," *J. Quant. Spectrosc. Radiat. Transfer* **104**(3), 450–459 (2007), <http://dx.doi.org/10.1016/j.jqsrt.2006.09.013>.
17. H. Matsueda, H. Y. Inoue, and M. Ishii, "Aircraft observation of carbon dioxide at 8–13 km altitude over the western Pacific from 1993 to 1999," *Tellus, Ser. B* **54**(1), 1–21 (2002), <http://dx.doi.org/10.1034/j.1600-0889.2002.00304.x>.
18. W. Bai, X. Zhang, and P. Zhang, "Temporal and spatial distribution of tropospheric CO<sub>2</sub> over China based on satellite observations," *Chin. Sci. Bull.* **55**(31), 3612–3618 (2010), <http://dx.doi.org/10.1007/s11434-010-4182-4>.
19. H. H. Aumann et al., "AIRS/AMSU/HSB on the aqua mission: design, science objectives, data products, and processing systems," *IEEE Trans. Geosci. Remote Sens.* **41**(2), 253–264 (2003), <http://dx.doi.org/10.1109/TGRS.2002.808356>.
20. E. T. Olsen, *AIRS/AMSU/HSB Version 5 Data Release User Guide*, Jet Propulsion Laboratory, California Institute of Technology, Pasadena, California (2007).
21. S. A. Clough et al., "Atmospheric radiative transfer modeling: a summary of the AER codes, Short Communication," *J. Quant. Spectrosc. Radiat. Transfer* **91**(2), 233–244 (2005), <http://dx.doi.org/10.1016/j.jqsrt.2004.05.058>.
22. L. S. Rothmana et al., "Rayleigh-scattering calculations for the terrestrial atmosphere," *Appl. Opt.* **34**(15), 2765–2773 (1995), <http://dx.doi.org/10.1364/AO.34.002765>.
23. A. Bucholtz, "The HITRAN 2008 molecular spectroscopic database," *J. Quant. Spectrosc. Radiat. Transfer* **110**(9–11), 533–572 (2009), <http://dx.doi.org/10.1016/j.jqsrt.2009.02.013>.
24. E. T. Olsen, *AIRS Version 5 Release Tropospheric CO<sub>2</sub> Products*, Jet Propulsion Laboratory, California Institute of Technology, Pasadena, California (2009).
25. K. A. Boering et al., "Stratospheric mean ages and transport rates from observations of carbon dioxide and nitrous oxide," *Science* **274**(5291), 1340–1343 (1996), <http://dx.doi.org/10.1126/science.274.5291.1340>.
26. D. Waugh and T. Hall, "Age of stratospheric air: theory, observations, and models," *Rev. Geophys.* **40**(4), 1–26 (2002), <http://dx.doi.org/10.1029/2000RG000101>.
27. C. G. Morgan et al., "Isotopic fractionation of nitrous oxide in the stratosphere: Comparison between model and observations," *J. Geophys. Res.* **109**(4), D04305 (2004), <http://dx.doi.org/10.1029/2003JD003402>.
28. R. L. Shia et al., "CO<sub>2</sub> in the upper troposphere: influence of stratosphere-troposphere exchange," *Geophys. Res. Lett.* **33**(1), L14814 (2006), <http://dx.doi.org/10.1029/2006GL026141>.
29. K. Bramstedt et al., "Comparison of total ozone from the satellite instruments GOME and TOMS with measurements from the Dobson network 1996–2000," *Atmos. Chem. Phys. Discuss.* **3**(5), 1409–1419 (2003), <http://dx.doi.org/10.5194/acpd-2-1131-2002>.
30. E. Fetzer, *Validation of AIRS/AMSU/HSB Core Products for Data Release Version 3.0*, Jet Propulsion Laboratory, California Institute of Technology, Pasadena, California (2003).
31. G. Grieco et al., "IMG O<sub>3</sub> retrieval and comparison with TOMS/ADEOS columnar ozone: an analysis based on tropical soundings," *J. Quant. Spectrosc. Radiat. Transfer* **95**(3), 331–348 (2005), <http://dx.doi.org/10.1016/j.jqsrt.2004.11.016>.

**Mandi Zhou** received her PhD from East China Normal University in 2013. She received her BS and MS in information and computing science from China University of Geosciences in 2006 and 2009, respectively. Her research interests include hyperspectral remote sensing and image processing.

**Jiong Shu** is currently a professor of climatology at the Key Laboratory of Geographic Information Science, East China Normal University. He received his MS and PhD from East China Normal University. He was an honor research fellow at the University of Liverpool,



UK, in 1999, after which he was employed as a professor at the College of Resources and Environmental Science, East China Normal University, in 2000. His research interests include climate change and environmental remote sensing.

**Ci Song** is a PhD candidate at East China Normal University. She received her BS from Henan Normal University in 2008 and MS in mathematics and applied mathematics from East China Normal University in 2011. Her research interests include differential equations and atmospheric remote sensing.

**Wei Gao** is a Changjiang scholar lecturing professor of the College of Resources and Environmental Science, East China Normal University, and professor in the Department of Ecosystem Science and Sustainability, Colorado State University. He received his PhD from Purdue University and had his postdoctoral training at the National Center for Atmospheric Research. His research interests include atmospheric radiation, remote sensing applications, regional climate/ecosystem modeling, geographic information systems. He is a fellow of SPIE.